

**MINOS and  $CPT$ -violating neutrinos**

Gabriela Barenboim\*

*Departament de Física Teòrica and IFIC, Universitat de València-CSIC Carrer Dr. Moliner 50, E-46100 Burjassot (València), Spain*

Joseph D. Lykken†

*Fermi National Accelerator Laboratory, P. O. Box 500, Batavia, Illinois 60510, USA*

(Received 28 October 2009; published 21 December 2009)

We review the status of  $CPT$  violation in the neutrino sector. Apart from LSND, current data favors three flavors of light stable neutrinos and antineutrinos, with both halves of the spectrum having one smaller mass splitting and one larger mass splitting. Oscillation data for the smaller splitting are consistent with  $CPT$ . For the larger splitting, current data favor an antineutrino mass-squared splitting that is an order of magnitude larger than the corresponding neutrino splitting, with the corresponding mixing angle less than maximal. This  $CPT$ -violating spectrum is driven by recent results from MINOS, but is consistent with other experiments if we ignore LSND. We describe an analysis technique which, together with MINOS running optimized for muon antineutrinos, should be able to conclusively confirm the  $CPT$ -violating spectrum proposed here, with as little as 3 times the current data set. If confirmed, the  $CPT$ -violating neutrino mass-squared difference would be an order of magnitude less than the current most-stringent upper bound on  $CPT$  violation for quarks and charged leptons.

DOI: 10.1103/PhysRevD.80.113008

PACS numbers: 14.60.Pq, 11.30.Er

**I. INTRODUCTION**

All known particles are either self-conjugate under  $CPT$  or have  $CPT$  conjugate “antiparticles.” In every case the antiparticle partner is observed to have the same mass as the corresponding particle, within experimental resolutions. These observations are consistent with the description of all nongravitational particle interactions by local relativistic quantum field theory, where  $CPT$  conservation is a result of the intimate connection between Lorentz invariance, locality, Hermiticity, and the absence of operator-ordering ambiguities. For precisely this reason it is important to pursue increasingly rigorous tests of  $CPT$  invariance, and to extend our experimental constraints to sectors previously beyond reach.

In this regard neutrinos are especially interesting. Neutrinos have tiny nonzero masses, suggesting that the neutrino mass generation mechanism has novel features and that neutrinos communicate to a sector of new physics whose effects on charged leptons and quarks are as yet unobservable. As demonstrated in the next section, the current generation of neutrino oscillation experiments is sensitive to  $CPT$ -violating effects orders of magnitude smaller than what so far could have been detected for charged leptons or quarks. There is both theoretical and experimental motivation to pursue a rigorous study of  $CPT$  properties for neutrinos, keeping in mind that  $CPT$  violation may correlate with other exotic effects such as Lorentz violation or quantum decoherence.

In this paper we update [1–8] the experimental constraints on  $CPT$  violation for neutrinos, focusing on the case where other new physics effects are subdominant to a  $CPT$ -violating difference in neutrino/antineutrino mass spectra. As favored by the data we also assume three flavors of light stable neutrinos and antineutrinos, both halves of the spectrum having one smaller “solar” mass difference and one larger “atmospheric” mass difference. For the larger splitting we show that the global data set favors an antineutrino mass-squared splitting that is an order of magnitude larger than the corresponding neutrino splitting, as well as an antineutrino mixing angle  $\bar{\theta}_{23}$  that is less than maximal. This  $CPT$ -violating spectrum is driven by recent results from MINOS [9], but is consistent with other experiments.

We describe an analysis technique to confirm or deny the best-fit  $CPT$ -violating hypothesis with future data. We advocate and demonstrate the use of the Neyman-Pearson hypothesis test [10], also known as the  $\alpha$ - $\beta$  test, generalized from ratios of simple likelihoods to ratios of extended likelihoods with floating parameters. This method has the advantage, for a given likelihood ratio, of distinguishing between the test significance  $\alpha$ , the probability that  $CPT$ -conserving masses and mixings are rejected even though they are in fact correct, and the power of the test  $1 - \beta$ , where  $\beta$  is the probability that the  $CPT$ -violating solution is rejected even though it is in fact correct. For a given future data set, one can require that the  $p$ -value of the  $CPT$ -conserving hypothesis as extracted from the likelihood ratio is less than some benchmark significance  $\alpha$  chosen according to one’s theoretical prejudice about  $CPT$  violation.

\*gabriela.barenboim@uv.es

†lykken@fnal.gov

In advance of new data we can use Monte Carlo experiments to extract the value of  $\beta$ , thus estimating the prospects for distinguishing *CPT* violation in the neutrino spectrum if it is in fact present. We examine these prospects for the MINOS experiment. To be conservative, in maximizing the likelihoods we do not float parameters defining the *CPT*-violating mass spectrum, since this would tend to increase the maximum likelihood for the *CPT*-violating hypothesis even when it is wrong. We do however float experimental parameters related to the overall neutrino production rate and the energy spectrum; floating these parameters increases the maximum likelihoods for the incorrect hypotheses while leaving the maximum likelihoods for the correct hypotheses essentially unchanged, thus lessening the power of the Neyman-Pearson test.

Even with this conservative approach, we demonstrate that MINOS running optimized for muon antineutrinos should be able to conclusively confirm the *CPT*-violating spectrum proposed here, with as little as 3 times the current data set.

## II. *CPT* VIOLATION IN THE NEUTRINO SECTOR

### A. *CPT* violation with and without Lorentz violation or other exotic new physics

The discovery of parity (*P*) violation in fundamental interactions was a big surprise, especially considering that *P* is an element of the extended Lorentz group. As we now understand, it is possible to violate *P* in quantum field theory without compromising invariance under the restricted Poincaré group that includes only proper orthochronous Lorentz transformations, i.e. Lorentz transformations continuously connected to the identity.

For *CPT*, the connection to Lorentz invariance is even stronger. As emphasized by Feynman, in a local description of quantum field theory the Lorentz invariance of off-shell amplitudes requires combining processes with propagation of both off-shell states and *CPT* conjugates of those states. Going the other way, Greenberg has shown [11] that in quantum field theory *CPT*-violating mass differences on-shell inevitably lead to Lorentz-breaking effects off-shell, with consequences for both locality and operator-ordering in quantum field theory.

Because of the intimate theoretical connection between *CPT* and Lorentz invariance, experimental searches for *CPT* violation are related to experimental tests of Lorentz invariance. In both cases the most straightforward experimental approach is to look for departures from the expected relativistic on-shell dispersion relations for particles and antiparticles:

$$E^2 = \vec{p}^2 + m^2, \quad \bar{E}^2 = \vec{\bar{p}}^2 + \bar{m}^2, \quad \bar{m} = m, \quad (2.1)$$

where here and throughout a bar denotes a quantum num-

ber of a *CPT* conjugate state. This relationship suggests three experimentally distinct scenarios:

- (i) Detectable violations of Lorentz invariance in the dispersion relations for some particles, but conserving *CPT* to within experimental resolutions.
- (ii) Detectable violations of Lorentz invariance in the dispersion relations for some particles, accompanied also by detectable violations of *CPT*.
- (iii) Detectable violations of *CPT* in the dispersion relations for some particles, but conserving Lorentz invariance to within experimental resolutions.

The first two scenarios are motivated by the possibility of a spontaneous breaking of vacuum Lorentz invariance, perhaps related to new Planckian physics such as space-time foam, superstrings, or extra dimensions [12–22]. The third scenario is motivated by the possibility of nonlocal physics whose primary on-shell effect may be *CPT* violation [23].

A further complication is that exotic new physics such as quantum decoherence [12–14] or extra dimensions [21] may lead to baseline-dependent effects on neutrino oscillations with additional *CPT*-violating features not captured by deviations from the expected dispersion relations. Of course matter effects, though predicted by the standard model, are also an example of baseline-dependent effects on neutrino oscillations with *CPT*-violating features.

For neutrino oscillation experiments there are thus effectively three kinds of tests of *CPT*:

- (1) Searches for Lorentz-violating effects in concert with *CPT* violation. The current best limits on this case are from the MINOS experiment [24]; we will not elaborate further on this scenario.
- (2) Searches for *CPT*-violating differences between neutrino and antineutrino mass spectra. This is the main subject of our paper.
- (3) Searches for inconsistencies in oscillation results that could signal baseline-dependent new physics with possible ramifications for *CPT*. Prospective limits are discussed in [16,19,21].

In the last case there is an important connection between *CP* and *CPT*. Even when *CPT* is conserved, *CP* violation in neutrino mixing allows the possibility of differences between neutrino and antineutrino oscillation probabilities in neutrino *appearance* experiments:

$$P(\nu_a \rightarrow \nu_b) \neq P(\bar{\nu}_a \rightarrow \bar{\nu}_b). \quad (2.2)$$

However, as shown in [4], *CP* violation without *CPT* violation cannot produce a neutrino-antineutrino discrepancy in *disappearance* experiments:

$$P(\nu_a \rightarrow \nu_\mu) \neq P(\bar{\nu}_a \rightarrow \bar{\nu}_\mu). \quad (2.3)$$

A corollary of these results is that a neutrino-antineutrino oscillation discrepancy arising from *CP* violation without

*CPT* violation requires at least two relevant mass splittings contributing to the oscillation, as occurs e.g. in some (3 + 2) sterile neutrino models [25].

### B. Comparing limits on *CPT* violation

Assuming that the source of *CPT* violation is a mass asymmetry in the dispersion relations (2.1), the relevant figure of merit in comparing different experimental limits on *CPT*-violation is the mass-squared difference between a particle and its *CPT* conjugate.

For quarks the most stringent experimental limit [26] is from neutral kaons, whose mass-squared difference is constrained to be less than  $0.5 \text{ eV}^2$ , or  $\sim 0.1 \text{ eV}^2$  if we attribute the *CPT* asymmetry to the constituent strange quarks.

For charged leptons, the most stringent constraint [26] is from the upper limit on the electron-positron mass difference; this corresponds to an upper bound on the mass-squared difference of approximately  $2 \times 10^4 \text{ eV}^2$ .

The *CPT*-violating best fit reported here corresponds to a difference of mass-squared differences of only  $0.02 \text{ eV}^2$ . This means that for neutrinos the current generation of oscillation experiments has sensitivities to potential *CPT*-violating effects orders of magnitude smaller than the above limits. Note that Bahcall *et al.* reached the same conclusion applying different figures of merit [27] (see also [28,29]).

Thus, contrary to what is sometimes implied in the literature, it is plausible that *CPT*-violating mass differences would be detected first in the neutrino sector, even if such effects have comparable magnitude in the quark and charged lepton sectors. Furthermore, as noted already in the introduction, since neutrinos appear to gain mass through a novel mechanism, it is also plausible that *CPT*-violating mass differences are much larger for neutrinos compared to the other sectors.

### III. *CPT*-VIOLATING NEUTRINO MASS SPECTRA

The main constraints on the mass differences and mixings of neutrinos come from the neutrino oscillation experiments [30–44] summarized in Table I.

Because we are interested in the possibility of *CPT* violation, we will consider the masses and mixings of the neutrino mass matrix as completely independent of the masses and mixings of the antineutrino mass matrix, and consider the experimental constraints on each matrix separately. Because of the flavor sensitivity of the SNO results, the active neutrino composition of the solar neutrino oscillation is well-constrained. The Super-Kamiokande data also have some flavor sensitivity; technically this measures the sum of the atmospheric neutrino and antineutrino oscillations, but in practice is mostly constraining for the neutrinos, which dominate over the antineutrinos as cosmic ray secondaries in the relevant energy range. The Super-Kamiokande atmospheric neutrino data are bolstered by accelerator-based experiments K2K and MINOS, which report muon neutrino disappearance consistent with the atmospheric mass splitting and large mixing. The net result [45] is that the active neutrino masses and mixings are required to closely resemble the left half of the spectrum shown in Fig. 1, modulo the possibility of inverting the solar-atmospheric hierarchy. The main question on the neutrino side is whether there are small admixtures of one or more sterile neutrinos in the three light mass eigenstates, but as yet there is no evidence for such mixings.

On the antineutrino side, the situation is less clear. KamLAND has reported an electron antineutrino disappearance signal consistent with an antineutrino mass splitting and mixings equivalent to the solar counterpart on the neutrino side. LSND reported a  $\bar{\nu}_\mu \rightarrow \bar{\nu}_e$  appearance signal consistent with an antineutrino mass-squared splitting

TABLE I. Summary of current and past neutrino oscillation experiments. The first column shows the principle oscillations that the experiment could in principle observe; the second column indicates whether this constitutes an appearance (app) or disappearance (dis) experiment. The third column indicates the primary sensitivity, either to solar mass splittings, atmospheric (atm), or short-baseline (SBL).

CHOOZ [30], Bugey [31], Palo Verde [32]	$\bar{\nu}_e \rightarrow \bar{\nu}_\mu$	dis	SBL
CDHS [33], CCFR [34]	$\nu_\mu \rightarrow \nu_\mu$	dis	SBL
NOMAD [35]	$\nu_\mu \rightarrow \nu_e$	app	SBL
LSND [36], KARMEN [37]	$\bar{\nu}_\mu \rightarrow \bar{\nu}_e$	app	SBL
MiniBooNE [38]	$\nu_\mu \rightarrow \nu_e$	app	SBL
Super-Kamiokande [39]	$(\nu_\mu \rightarrow \nu_\mu) + (\bar{\nu}_\mu \rightarrow \bar{\nu}_\mu)$	dis	atm
K2K [40]	$\nu_\mu \rightarrow \nu_\mu$	dis	atm
MINOS [41]	$\nu_\mu \rightarrow \nu_\mu$	dis	atm
SNO [42]	$\bar{\nu}_\mu \rightarrow \bar{\nu}_\mu$		
	$\nu_e \rightarrow \nu_\mu$	dis	solar
	$\nu_e \rightarrow \nu_\tau$		
Borexino [43]	$\nu_e \rightarrow \nu_\mu$	dis	solar
KamLAND [44]	$\bar{\nu}_e \rightarrow \bar{\nu}_\mu$	dis	solar

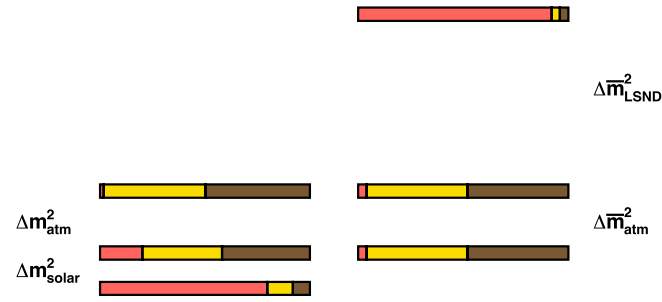


FIG. 1 (color online). The  $CPT$ -violating neutrino spectrum proposed in [2] as an explanation of LSND.

$\sim 1 \text{ eV}^2$ . MINOS has reported preliminary muon antineutrino disappearance results, consistent with an antineutrino mass-squared splitting that is roughly the geometric mean of the KamLAND and LSND favored splittings.

Thus, even allowing for  $CPT$  violation, oscillations between three active antineutrino species cannot reconcile KamLAND, MINOS, and LSND simultaneously. The  $CPT$ -violating spectrum shown in Fig. 1, proposed in [2] to accommodate solar, atmospheric, and LSND splittings with only three active flavors, was conclusively excluded by KamLAND [6].

Without resorting to new baseline-dependent exotic physics, this leaves two possibilities:

Case (i).—The LSND results are incorrect.

Case (ii).—The LSND results are correct, but the corresponding short-baseline (SBL) oscillation involves mixing with one or more species of sterile neutrinos.

In the second case one may question whether it is even necessary to resort to a  $CPT$ -violating mass spectrum, since the addition of sterile neutrinos adds new parameters that potentially loosen up the experimental constraints. Several recent analyses [25,46–48] have looked at this question in detail, using global fits that (in the case of [48]) include the latest MiniBooNE data. The conclusion is that  $CPT$ -conserving sterile neutrino scenarios, even allowing for the possibility of large  $CP$  violation in the case of two or more sterile species, cannot avoid at least a  $3\sigma$  discrepancy among different experimental data sets, with the largest tension between the SBL appearance experiments and the SBL disappearance experiments.

Thus case (ii) requires either that we disregard some oscillation results other than LSND, or that we again resort to a  $CPT$ -violating spectrum. Thus, for example, one could develop  $CPT$ -violating versions of the  $3 + 2$  spectrum shown in Fig. 2. We will not pursue this possibility further here, since it is already under investigation elsewhere [49].

The remainder of this paper is devoted to case (i): we disregard the LSND signal, and explore to what extent a  $CPT$ -violating neutrino spectrum is allowed, or even favored, by the remaining global data set. For simplicity we will assume that the situation is not further complicated by

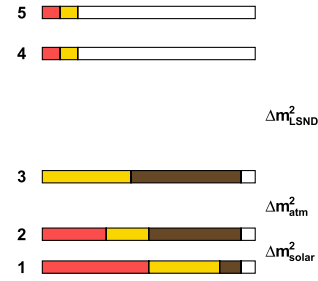


FIG. 2 (color online). The  $3 + 2$   $CPT$ -conserving but potentially  $CP$ -violating neutrino spectrum proposed in [25] attempting to reconcile LSND, MiniBooNE, and other short-baseline oscillation results.



FIG. 3 (color online). The best-fit  $CPT$ -violating neutrino spectrum obtained from our analysis.

sterile neutrinos or baseline-dependent exotic physics, though of course both are possible.

With these assumptions there is qualitatively only one  $CPT$ -violating neutrino mass spectrum candidate, shown in Fig. 3 and first discussed in [6]. To be more precise there are four candidate spectra, since we can invert the hierarchy on either the neutrino or antineutrino side independently, but existing data are insensitive to these choices, with the exception of the neutrino observations from supernova SN1987A [1].

As discussed above, the neutrino side of the spectrum in Fig. 3 is completely constrained by data. On the antineutrino side, the smaller solar mass splitting is necessary to accommodate the KamLAND signal; a  $CPT$ -violating variation of this splitting and the related mixings is still allowed at about the 5% level. The larger mass splitting has to accommodate the antineutrino disappearance signals from MINOS and Super-Kamiokande, the null appearance results from KARMEN and MiniBooNE, as well as the null disappearance results from other SBL oscillation experiments.

#### IV. CONSTRAINING THE ANTINEUTRINO SPECTRUM

To make detailed contact with the experimental results we first introduce the neutrino survival and transition probabilities given by

$$P(\nu_\alpha \rightarrow \nu_\beta) = \delta_{\alpha\beta} - 4 \sum_{i>j=1}^3 U_{\alpha i} U_{\beta i} U_{\alpha j} U_{\beta j} \sin^2 \left[ \frac{\Delta m_{ij}^2 L}{4E} \right] \quad (4.1)$$

for neutrinos and

$$P(\bar{\nu}_\alpha \rightarrow \bar{\nu}_\beta) = \delta_{\alpha\beta} - 4 \sum_{i>j=1}^3 \bar{U}_{\alpha i} \bar{U}_{\beta i} \bar{U}_{\alpha j} \bar{U}_{\beta j} \sin^2 \left[ \frac{\Delta \bar{m}_{ij}^2 L}{4E} \right] \quad (4.2)$$

$$U = \begin{pmatrix} c_{12}c_{13} & s_{12}c_{13} & s_{13} \\ -s_{12}c_{23} - c_{12}s_{23}s_{13} & c_{12}c_{23} - s_{12}s_{23}s_{13} & s_{23}c_{13} \\ s_{12}s_{23} - c_{12}c_{23}s_{13} & -c_{12}s_{23} - s_{12}c_{23}s_{13} & c_{23}c_{13} \end{pmatrix} \quad (4.4)$$

and similarly for  $\bar{U}$ . In Eq. (4.1)  $L$  denotes the distance between the neutrino source and the detector, and  $E$  is the lab energy of the neutrino.

We use the notation  $\Delta m_{\text{solar}}^2 = \Delta m_{12}^2$ ,  $\Delta m_{\text{atm}}^2 = \Delta m_{13}^2$  to denote the smaller and larger mass-squared splittings on the neutrino side, and  $\Delta \bar{m}_{\text{solar}}^2 = \Delta \bar{m}_{12}^2$ ,  $\Delta \bar{m}_{\text{atm}}^2 = \Delta \bar{m}_{13}^2$  for the antineutrinos.

SBL reactor experiments give important constraints on the antineutrino spectrum. Their results indicate [30–32] that electron antineutrinos produced in reactors remain electron antineutrinos on short baselines. Because of the short baselines we can ignore the smallest (solar) antineutrino mass difference and average the other two; the survival probability can be expressed as

$$P(\bar{\nu}_e \rightarrow \bar{\nu}_e) = 1 - 2\bar{U}_{e3}^2(1 - \bar{U}_{e3}^2). \quad (4.5)$$

Thus, even for rather large antineutrino mass differences, the survival probability will be close to 1 if  $\bar{U}_{e3}$  is either

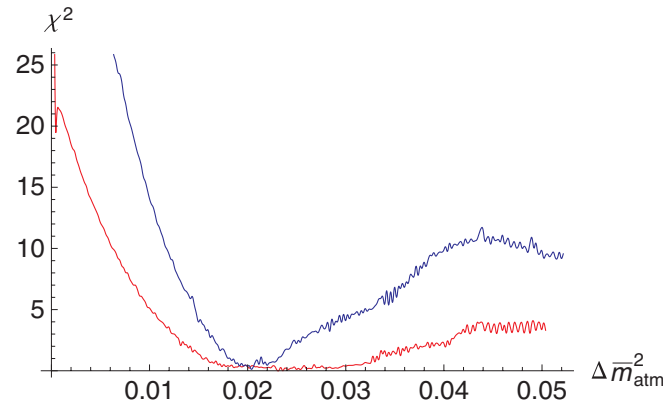


FIG. 4 (color online). The relative  $\chi^2$  deviation of the *CPT*-violating fit to data from MINOS, Super-Kamiokande, KamLAND, and CHOOZ, as a function of the single parameter  $\Delta \bar{m}_{\text{atm}}^2$  (in  $\text{eV}^2$ ), with  $\sin^2 \bar{\theta}_{23} = 0.407$ . The lower (red) curve excludes the MINOS muon antineutrino data, while the upper (blue) curve includes them.

for antineutrinos. The matrix  $U = \{U_{\alpha i}\}$  ( $\bar{U} = \{\bar{U}_{\alpha i}\}$ ) describes the weak interaction neutrino (antineutrino) states,  $\nu_\alpha$ , in terms of the neutrino (antineutrino) mass eigenstates,  $\nu_i$ . That is,

$$\nu_\alpha = \sum_i U_{\alpha i} \nu_i \quad \text{and} \quad \bar{\nu}_\alpha = \sum_i \bar{U}_{\alpha i} \bar{\nu}_i, \quad (4.3)$$

where we have ignored the possible *CP* phases. The matrices can be parametrized as follows:

almost 1 or almost 0. Physically this means that we can choose between having almost all the antielectron flavor in the heavy state (which really means the furthest-away state since we can invert the spectrum) or alternatively leave this state with almost no antielectron flavor. The first possibility was depicted in the Fig. 1, while the second is realized in Fig. 3.

MINOS and Super-Kamiokande constrain both the larger antineutrino mass-squared difference  $\Delta \bar{m}_{\text{atm}}^2$  and the antineutrino mixing angle  $\bar{\theta}_{23}$ . KamLAND constrains mostly the smaller antineutrino mass-squared difference  $\Delta \bar{m}_{\text{solar}}^2$ .

We have performed a  $\chi^2$  fit of the antineutrino spectrum (assuming three active flavors only) using the data from MINOS, Super-Kamiokande, KamLAND, and CHOOZ. The best-fit result is shown in Fig. 3. The *CPT*-violating features are encapsulated in

$$\Delta \bar{m}_{\text{atm}}^2 = 0.02 \text{ eV}^2, \quad \sin^2 \bar{\theta}_{23} = 0.407, \quad (4.6)$$

compared to the global-fit neutrino spectrum values

$$\Delta \bar{m}_{\text{atm}}^2 = 0.0025 \text{ eV}^2, \quad \sin^2 \theta_{23} = 0.707. \quad (4.7)$$

This *CPT* violation is driven by the MINOS results; indeed our best-fit values for  $\Delta \bar{m}_{\text{atm}}^2$  and  $\sin^2 2\bar{\theta}_{23}$  are close to those reported by MINOS fitting their data alone.

The overall quality of our fit is good, with a  $\chi^2$  per degree of freedom of 0.98. As seen in Fig. 4, the  $\chi^2$  deviation as a function of the single variable  $\Delta \bar{m}_{\text{atm}}^2$  has a clearly defined minimum. We note however that this is only the case when  $\bar{\theta}_{23}$  is allowed to float in the fit; if  $\bar{\theta}_{23}$  were fixed to maximal mixing, then the chi-squared distribution in  $\Delta \bar{m}_{\text{atm}}^2$  would be rather flat.

## V. DISCUSSION AND FUTURE PROSPECTS

The MINOS muon antineutrino disappearance results should be regarded as preliminary. They are from data runs with the target optimized for neutrinos, introducing more complicated systematics for the antineutrinos, and

poorer statistics (42 events observed at the far detector). This situation will improve dramatically with results from MINOS running optimized for antineutrinos, scheduled to begin soon.

Our fit shows that large, order-of-magnitude  $CPT$  violation in the neutrino sector is still a viable possibility. Making the further assumptions that the  $CPT$  violation is (approximately) baseline-independent and does not have a strong dependence on sterile mixing, a unique  $CPT$ -violating mass and mixing pattern is selected, up to the four-fold ambiguity of inverting the neutrino and/or antineutrino hierarchies.

The most timely question is whether better data in the near future from MINOS could provide compelling evidence for neutrino  $CPT$  violation. To address this question, we have performed toy muon antineutrino disappearance experiments, using the survival probability obtained either from a  $CPT$ -conserving spectrum or from our best-fit  $CPT$ -violating spectrum. We use the reconstructed muon antineutrino energy spectrum reported by MINOS, but to add some realism we allow a one-parameter distortion of the energy spectrum, and float this parameter in the fit. We also float  $N_0$ , the mean expected number of neutrinos detected in the MINOS far detector in the absence of oscillations; while this number is estimated in the experiment, it is subject to significant systematic uncertainty. We also float  $N_{\text{osc}}$ , the actual (but unmeasured) number of neutrinos in each experiment that would have been detected had they not oscillated to a different neutrino flavor.

Each toy experiment is equivalent to MINOS running with 200 nominal muon antineutrino events expected in the far detector in the absence of oscillations. This is approximately a factor of 3 increase over the current data. For each of 300 000 toy experiments based on each mass spectrum, we compute the maximum likelihood (i.e. we maximize the likelihood with respect to the floated parameters) for both  $CPT$ -conserving and  $CPT$ -violating hypotheses; then we plot the normalized distribution of events versus the logarithm of the ratio of the likelihoods. The definition of the likelihood and the details of the analysis are presented in the Appendix. The result is shown in Fig. 5.

This plot allows a Neyman-Pearson test of the  $CPT$ -conserving versus  $CPT$ -violating hypotheses. We choose a cut  $\alpha$  on the log ratio of the likelihoods for the case that the toys are based on the  $CPT$ -conserving spectrum; the significance  $\alpha$  corresponds to the probability that the  $CPT$ -conserving hypothesis is rejected even though it is true. Clearly we should choose a small value for  $\alpha$ , since we have a strong prior bias that  $CPT$  is conserved. Having thus fixed  $\alpha$  we can extract  $\beta$ , the probability that the  $CPT$ -conserving hypothesis is accepted even though the  $CPT$ -violating spectrum is the correct one. Then  $1 - \beta$  is the measure of the power of this hypothesis test.

The results are very encouraging: even with  $\alpha$  chosen as small as  $6 \times 10^{-7}$ , corresponding to a Gaussian signifi-

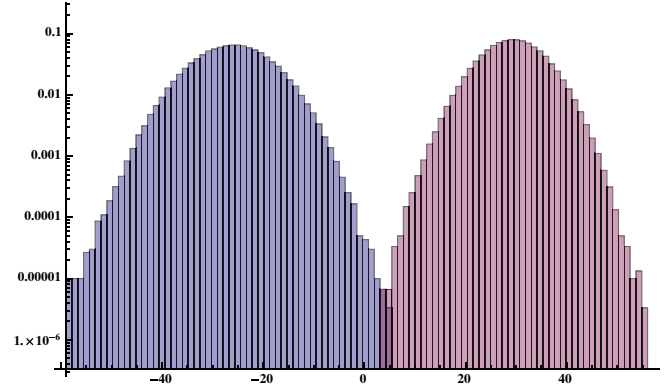


FIG. 5 (color online). The log likelihood ratio distribution for 300 000 toy experiments simulating 200 nominal muon antineutrinos per experiment on the MINOS baseline. The right-hand histogram uses the  $CPT$ -conserving hypothesis to generate the toy results, while the left-hand histogram uses the  $CPT$ -violating hypothesis. In both cases the ratio is from the maximum likelihood computed with the  $CPT$ -conserving PDFs over the maximum likelihood computed with the  $CPT$ -violating PDFs. The histograms are normalized to unit probability.

cance of  $5\sigma$ , we find  $1 - \beta$  very close to unity. This indicates a nearly 100% chance that the  $CPT$ -violating spectrum discussed in this paper would be correctly chosen by the hypothesis test if it is in fact true.

Figure 6 shows the oscillation probabilities of both the  $CPT$ -conserving and  $CPT$ -violating hypotheses plotted as a function of the muon antineutrino energy. The current MINOS data points (binned in energy) are superimposed. From this figure it is clear that the  $CPT$ -violating hypothesis makes clear energy-dependent predictions about what should be observed in future MINOS running:

- (i) The lowest energy bin will rise.
- (ii) The dip apparent to the eye around 10 GeV will remain.

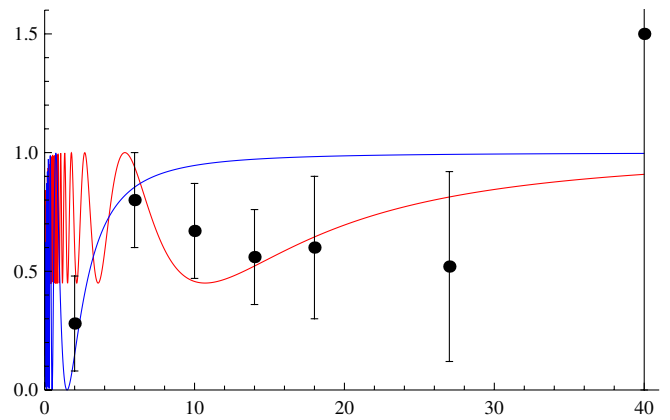


FIG. 6 (color online). Comparison of the binned MINOS muon antineutrino disappearance data with the oscillation curves obtained from the  $CPT$ -conserving hypothesis (blue) and the  $CPT$ -violating hypothesis (red).

This figure also explains why our prediction for the power of Neyman-Pearson test with 200 nominal MINOS events is so encouraging, even though we have very conservatively floated the total number of neutrinos in the likelihood fits. The discrimination of the *CPT*-conserving and *CPT*-violating hypotheses comes both from a significant difference in the overall survival probabilities and from the dramatic difference in the energy dependence of the survival probabilities. Even allowing for a rather large systematics, as we have done here, data generated from one hypothesis are almost never as well-described by the incorrect hypothesis, for experiments with at least 200 events.

### ACKNOWLEDGMENTS

The authors are grateful to Milind Diwan, Georgia Karagiorgi, Bill Louis, Olga Mena, Maurizio Pierini, Chris Quigg, and Chris Rogan, for useful discussions. G. B. acknowledges support from the Spanish MEC and FEDER under Contract No. FPA 2008/02878, and a Prometo grant. Fermilab is operated by the Fermi Research Alliance LLC under Contract No. DE-AC02-07CH11359 with the U.S. Department of Energy.

### APPENDIX: LIKELIHOOD METHODS AND NEUTRINO OSCILLATIONS

Consider a typical neutrino oscillation disappearance experiment, in which  $n_i$  neutrinos of a particular flavor are observed in a far detector in some number of energy bins labeled by  $i$ . Let  $N_s = \sum_i n_i$  be the total number of neutrinos observed, and for simplicity ignore the possibility of fakes or neutrinos from background sources.

Using observations in a near detector or some other method, one computes the mean number of neutrinos  $N_0$  that one would have expected to observe in the far detector in the absence of neutrino oscillations. For simplicity assume that  $N_0$  is the mean of a Poisson distribution, although one could also handle more complicated distributions. The experiment will also calculate the energy distribution of neutrinos expected at the far detector in the absence of oscillations. Both of the aforementioned distributions are hypotheses, perhaps with floating parameters representing uncertainties, but in both cases assume that the hypothetical distributions are independent of the particular neutrino oscillation model being tested.

Now suppose one has a hypothesis for the correct neutrino oscillation model. This amounts to specifying the particle distribution function (PDF)  $p_s(E)$ , the probability that a neutrino of energy  $E$  does not oscillate to a different flavor. Convoluting these PDFs with the energy distribution one obtains  $p_s^i$ , the probability that a neutrino is in the  $i$ th energy bin and did not oscillate. Letting  $p_s^{\text{total}} = \sum_i p_s^i$ , the probability that a given neutrino does oscillate to a different flavor is just  $p_{\text{osc}} = 1 - p_s^{\text{total}}$ .

The appropriate binned extended likelihood function given all these assumptions is given by

$$L = \frac{e^{-N_0} (N_0)^{N_s + N_{\text{osc}}}}{(N_s + N_{\text{osc}})!} \frac{(N_s + N_{\text{osc}})!}{N_s! N_{\text{osc}}!} p_{\text{osc}}^{N_{\text{osc}}} \prod_{i=1}^{N_{\text{osc}}} (p_s^i)^{n_i}, \quad (\text{A1})$$

where  $N_{\text{osc}}$  denotes the total number of neutrinos that oscillated to a different flavor.

In most applications of the extended likelihood formula, the analog of the total number of events, here  $N_s + N_{\text{osc}}$ , is known, while the mean expected number  $N_0$  is obtained from the fit by maximizing the likelihood. In the case at hand an estimate of  $N_0$  is already given,  $N_s$  is measured, and  $N_{\text{osc}}$  is unknown. Thus one would like to obtain  $N_{\text{osc}}$  by maximizing the likelihood. From the explicit dependence shown in (A1), it is easy to see that the likelihood is maximized by solving

$$\psi_0(N_{\text{osc}} + 1) = \log[N_0 p_{\text{osc}}], \quad (\text{A2})$$

where  $\psi_0$  is the digamma function.

For  $N_{\text{osc}} \geq 2$ , an excellent approximation to the solution of (A2) is given by

$$N_{\text{osc}} = N_0 p_{\text{osc}} - \frac{1}{2}. \quad (\text{A3})$$

Substituting back into (A1), we obtain an expression for the likelihood function already maximized with respect to the floating value of  $N_{\text{osc}}$ :

$$L = \frac{e^{-N_0} (N_0)^{N_s + N_0 p_{\text{osc}} - 1/2}}{N_s! \Gamma[N_0 p_{\text{osc}} + \frac{1}{2}]} p_{\text{osc}}^{N_0 p_{\text{osc}} - 1/2} \prod_{i=1}^{N_0 p_{\text{osc}} - 1/2} (p_s^i)^{n_i}. \quad (\text{A4})$$

This likelihood can then be further maximized with respect to other floating parameters.

In a real experiment the mean expected number  $N_0$  is estimated from other data with some error. If we take this error to be Gaussian, we can include this distribution in the definition of the extended likelihood, and maximize the likelihood with respect to both  $N_0$  and  $N_{\text{osc}}$ . The likelihood function becomes

$$L = \frac{\exp\left(-\frac{(N_0 - \bar{N}_0)^2}{2\sigma_{N_0}^2}\right)}{\sigma_{N_0} \sqrt{2\pi}} \times \frac{e^{-N_0} (N_0)^{N_s + N_0 p_{\text{osc}} - 1/2}}{N_s! \Gamma[N_0 p_{\text{osc}} + \frac{1}{2}]} p_{\text{osc}}^{N_0 p_{\text{osc}} - 1/2} \prod_{i=1}^{N_0 p_{\text{osc}} - 1/2} (p_s^i)^{n_i}, \quad (\text{A5})$$

where the parameters  $\bar{N}_0$  and  $\sigma_{N_0}$  are supposed to be fixed by, e.g., extrapolating from near detector data. In our fits we have used  $\bar{N}_0 = 200$  and  $\sigma_{N_0} = 20$ . We then maximize the likelihoods allowing  $N_0$  to take any value such that  $N_{\text{osc}}$  is nonnegative. This increases the maximized likelihood of the wrong hypothesis while having very little effect on the maximized likelihood for the correct hypothesis; thus floating the value of  $N_0$  decreases the log likelihood ratio of the correct hypothesis over the wrong hypothesis.

In our analysis we introduced a parameter  $c$  to represent uncertainty in the normalized energy distribution of neutrinos reaching the MINOS far detector:

$$p(E) = \frac{e^{-aE} E^b}{a^{-(b+1)} \Gamma[b+1]}, \quad a = 0.193489; \quad (A6)$$

$$b = 1.43356 + c,$$

where the numerical constants come from a fit to the MINOS spectrum. By allowing  $c$  to vary from  $-0.2$  to  $0.2$  in the fit independently for each neutrino oscillation hypothesis, we introduce a variability in the energy spectrum as illustrated in Fig. 7. This increases the maximized likelihood of the wrong hypothesis while having very little effect on the maximized likelihood for the correct hypothesis; thus allowing a distorted energy spectrum decreases the log likelihood ratio of the correct hypothesis over the wrong hypothesis.

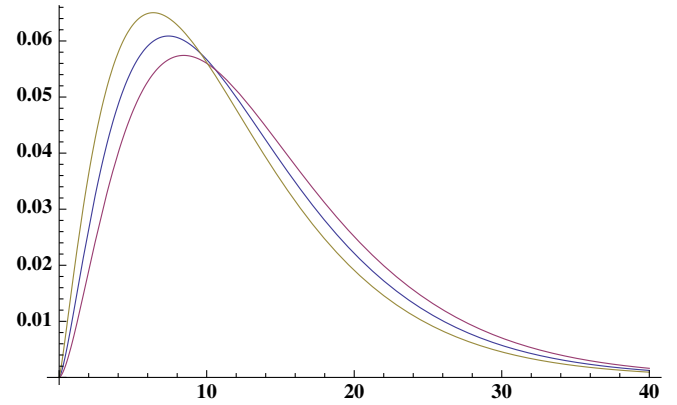


FIG. 7 (color online). The one-parameter variability in the normalized muon antineutrino energy spectrum floated in our maximum likelihood fits. The central (blue) curve is our best fit to the binned MINOS spectrum. The horizontal axis is energy in GeV.

- 
- [1] H. Murayama and T. Yanagida, *Phys. Lett. B* **520**, 263 (2001).
- [2] G. Barenboim, L. Borisso, J.D. Lykken, and A.Y. Smirnov, *J. High Energy Phys.* **10** (2002) 001.
- [3] S. Skadhauge, *Nucl. Phys.* **B639**, 281 (2002).
- [4] G. Barenboim, L. Borisso, and J.D. Lykken, *Phys. Lett. B* **534**, 106 (2002).
- [5] A. Strumia, *Phys. Lett. B* **539**, 91 (2002).
- [6] G. Barenboim, L. Borisso, and J.D. Lykken, arXiv:hep-ph/0212116.
- [7] M.C. Gonzalez-Garcia, M. Maltoni, and T. Schwetz, *Phys. Rev. D* **68**, 053007 (2003).
- [8] V.A. Kostelecky and M. Mewes, *Phys. Rev. D* **70**, 031902 (2004); **69**, 016005 (2004).
- [9] J. Hartnell *et al.* (MINOS Collaboration), “*Joint Experimental-Theoretical Seminar*,” Fermilab 2009 (unpublished).
- [10] F. James, *Statistical Methods in Experimental Physics* (World Scientific, Singapore, 2006), 2nd ed..
- [11] O.W. Greenberg, *Phys. Rev. Lett.* **89**, 231602 (2002).
- [12] G. Barenboim and N.E. Mavromatos, *J. High Energy Phys.* **01** (2005) 034.
- [13] G. Barenboim and N.E. Mavromatos, *Phys. Rev. D* **70**, 093015 (2004).
- [14] G. Barenboim, N.E. Mavromatos, S. Sarkar, and A. Waldron-Lauda, *Nucl. Phys.* **B758**, 90 (2006).
- [15] J. Bernabeu, J.R. Ellis, N.E. Mavromatos, D.V. Nanopoulos, and J. Papavassiliou, arXiv:hep-ph/0607322.
- [16] N.E. Mavromatos, A. Meregaglia, A. Rubbia, A. Sakharov, and S. Sarkar, *Phys. Rev. D* **77**, 053014 (2008).
- [17] N.E. Mavromatos, *Proc. Sci.*, KAON (2008) 041.
- [18] N.E. Mavromatos, arXiv:0906.2712.
- [19] A. Sakharov, N. Mavromatos, A. Meregaglia, A. Rubbia, and S. Sarkar, *J. Phys. Conf. Ser.* **171**, 012038 (2009).
- [20] S. Esposito and G. Salesi, arXiv:0906.5542.
- [21] S. Hollenberg, O. Micu, and H. Pas, *Phys. Rev. D* **80**, 053010 (2009); S. Hollenberg, O. Micu, H. Pas, and T.J. Weiler, *Phys. Rev. D* **80**, 053010 (2009); S. Hollenberg and H. Pas, arXiv:0904.2167.
- [22] J.S. Diaz, A. Kostelecky, and M. Mewes, *Phys. Rev. D* **80**, 076007 (2009).
- [23] G. Barenboim and J.D. Lykken, *Phys. Lett. B* **554**, 73 (2003).
- [24] P. Adamson *et al.* (MINOS Collaboration), *Phys. Rev. Lett.* **101**, 151601 (2008).
- [25] G. Karagiorgi, A. Aguilar-Arevalo, J.M. Conrad, M.H. Shaevitz, K. Whisnant, M. Sorel, and V. Barger, *Phys. Rev. D* **75**, 013011 (2007).
- [26] C. Amsler *et al.* (Particle Data Group), *Phys. Lett. B* **667**, 1 (2008).
- [27] J.N. Bahcall, V. Barger, and D. Marfatia, *Phys. Lett. B* **534**, 120 (2002).
- [28] S. Antusch and E. Fernandez-Martinez, *Phys. Lett. B* **665**, 190 (2008).
- [29] A. Dighe and S. Ray, *Phys. Rev. D* **78**, 036002 (2008).
- [30] M. Apollonio *et al.* (CHOOZ Collaboration), *Phys. Lett. B* **466**, 415 (1999).
- [31] Y. Declais *et al.*, *Nucl. Phys.* **B434**, 503 (1995).
- [32] F. Boehm *et al.*, *Phys. Rev. D* **64**, 112001 (2001).
- [33] F. Dydak *et al.*, *Phys. Lett.* **134B**, 281 (1984).
- [34] I.E. Stockdale *et al.*, *Phys. Rev. Lett.* **52**, 1384 (1984); K.S. McFarland *et al.*, *Phys. Rev. Lett.* **75**, 3993 (1995).
- [35] P. Astier *et al.* (NOMAD Collaboration), *Phys. Lett. B* **570**, 19 (2003).
- [36] C. Athanassopoulos *et al.* (LSND Collaboration), *Phys. Rev. Lett.* **77**, 3082 (1996); *Phys. Rev. C* **58**, 2489 (1998); A. Aguilar *et al.* (LSND Collaboration), *Phys. Rev. D* **64**, 112007 (2001).
- [37] B. Armbruster *et al.* (KARMEN Collaboration), *Phys. Rev. D* **65**, 112001 (2002).



- [38] A. A. Aguilar-Arevalo *et al.* (The MiniBooNE Collaboration), Phys. Rev. Lett. **98**, 231801 (2007); **102**, 101802 (2009); **103**, 111801 (2009).
- [39] Y. Ashie *et al.* (Super-Kamiokande Collaboration), Phys. Rev. Lett. **93**, 101801 (2004); J. Hosaka *et al.* (Super-Kamiokande Collaboration), Phys. Rev. D **74**, 032002 (2006).
- [40] M. H. Ahn *et al.* (K2K Collaboration), Phys. Rev. D **74**, 072003 (2006).
- [41] D. G. Michael *et al.* (MINOS Collaboration), Phys. Rev. Lett. **97**, 191801 (2006).
- [42] Q. R. Ahmad *et al.* (SNO Collaboration), Phys. Rev. Lett. **89**, 011301 (2002); **89**, 011302 (2002); B. Aharmim *et al.* (SNO Collaboration), Phys. Rev. C **72**, 055502 (2005).
- [43] C. Arpesella *et al.* (Borexino Collaboration), Phys. Lett. B **658**, 101 (2008); Phys. Rev. Lett. **101**, 091302 (2008); arXiv:0808.2868.
- [44] S. Abe *et al.* (KamLAND Collaboration), Phys. Rev. Lett. **100**, 221803 (2008).
- [45] M. C. Gonzalez-Garcia and M. Maltoni, Phys. Rep. **460**, 1 (2008).
- [46] M. Maltoni and T. Schwetz, Phys. Rev. D **76**, 093005 (2007).
- [47] A. Melchiorri, O. Mena, S. Palomares-Ruiz, S. Pascoli, A. Slosar, and M. Sorel, J. Cosmol. Astropart. Phys. 01 (2009) 036.
- [48] G. Karagiorgi, Z. Djurcic, J. M. Conrad, M. H. Shaevitz, and M. Sorel, Phys. Rev. D **80**, 073001 (2009).
- [49] Georgia Karagiorgi (private communication).